

SM Background in Rare B -Meson Decays

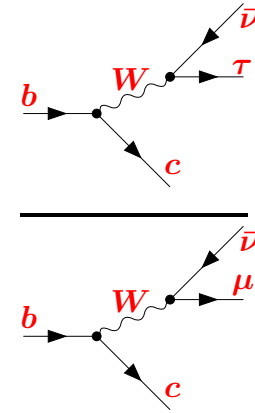
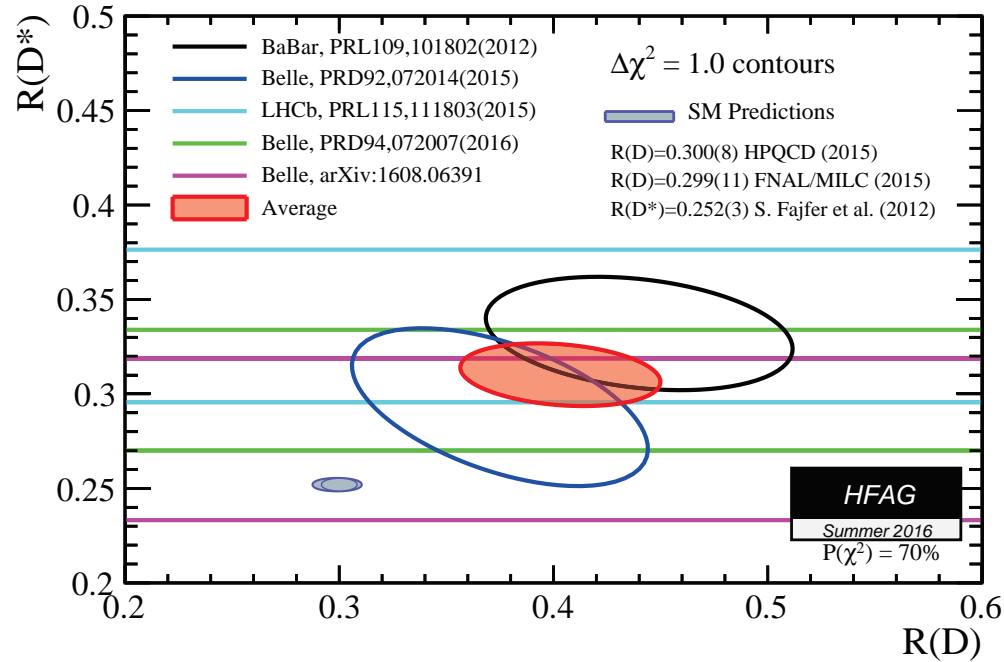
Mikołaj Misiak

University of Warsaw

HARMONIA meeting, April 26-30th 2018, Warsaw

1. B -physics “anomalies”
2. $\bar{B} \rightarrow X_s \gamma$ - progress in perturbative calculations
3. $B_{s,d} \rightarrow \ell^+ \ell^-$ - a phenomenological update
4. Charm-quark loops $\bar{B} \rightarrow X_s \ell^+ \ell^-$
5. Summary

$R(D)$ and $R(D^*)$ “anomalies” [HFAG, arXiv:1612.07233] (3.9σ)



$$R(D^{(*)}) = \mathcal{B}(B \rightarrow D^{(*)} \tau \bar{\nu}) / \mathcal{B}(B \rightarrow D^{(*)} \mu \bar{\nu})$$

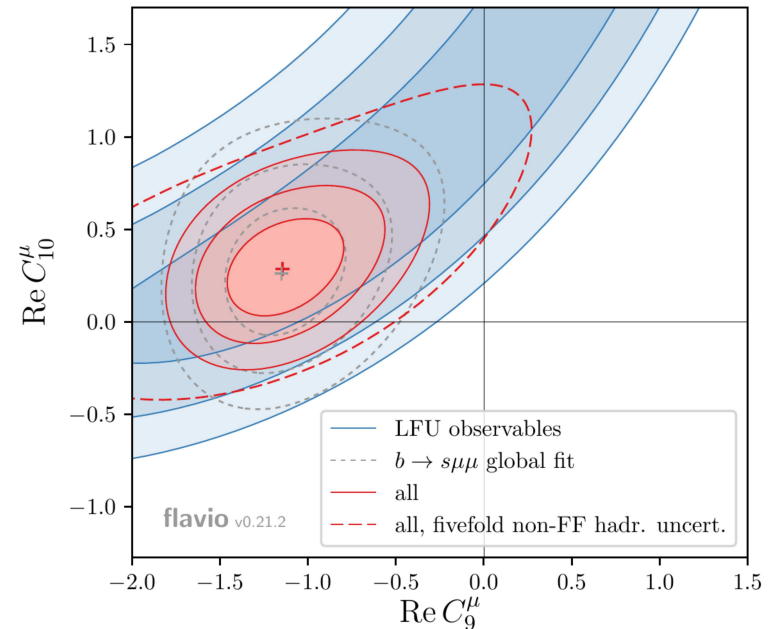
$b \rightarrow s \ell^+ \ell^-$ “anomalies” $(> 5\sigma)$

[W. Altmanshofer, February 2018, talk at the Munich workshop]

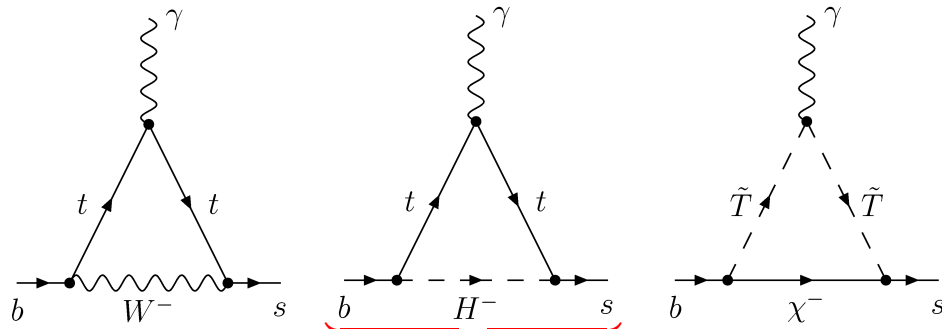
$$Q_9^\ell = \frac{\bar{l} \gamma_\alpha l}{b_L s_L} \text{ (diagram with } \gamma_\alpha \text{ vertex)}$$

$$Q_{10}^\ell = \frac{\bar{l} \gamma_\alpha \gamma_5 l}{b_L s_L} \text{ (diagram with } \gamma_\alpha \gamma_5 \text{ vertex)}$$

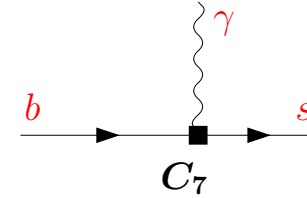
$\ell = e \text{ or } \mu$



Information on electroweak-scale physics in the $b \rightarrow s\gamma$ transition is encoded in an effective low-energy local interaction:

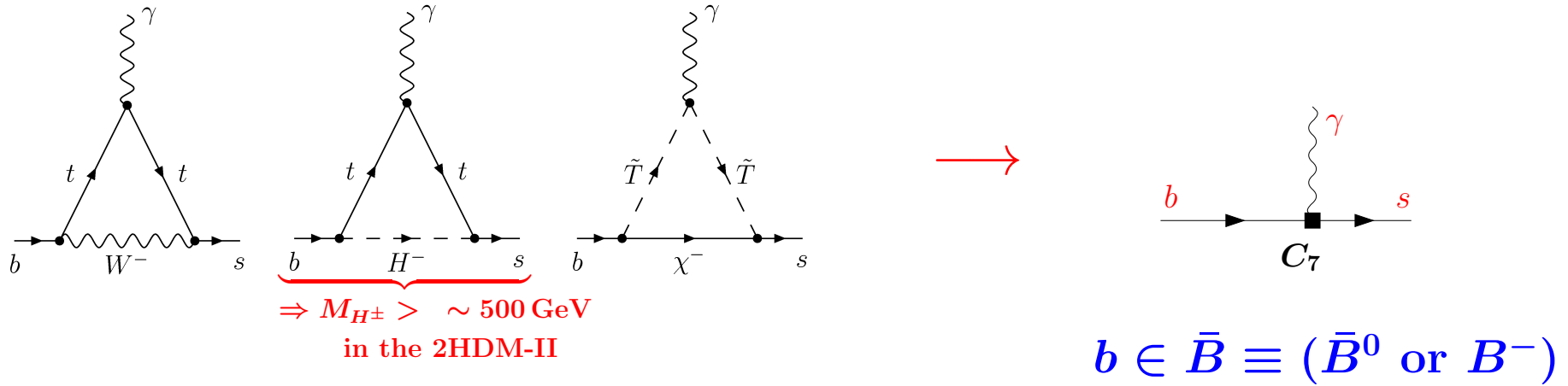


$\Rightarrow M_{H^\pm} > \sim 500 \text{ GeV}$
in the 2HDM-II



$b \in \bar{B} \equiv (\bar{B}^0 \text{ or } B^-)$

Information on electroweak-scale physics in the $b \rightarrow s\gamma$ transition is encoded in an effective low-energy local interaction:



The inclusive $\bar{B} \rightarrow X_s \gamma$ decay rate for $E_\gamma > E_0$ is well approximated by the corresponding perturbative decay rate of the b -quark:

$$\Gamma(\bar{B} \rightarrow X_s \gamma) = \Gamma(b \rightarrow X_s^p \gamma) + \left(\begin{array}{c} \text{non-perturbative effects} \\ (3 \pm 5)\% \end{array} \right)$$

[G. Buchalla, G. Isidori and S.-J. Rey, Nucl. Phys. B511 (1998) 594]
 [M. Benzke, S.J. Lee, M. Neubert and G. Paz, JHEP 1008 (2010) 099]
 (BLNP)

provided E_0 is large ($E_0 \sim m_b/2$)

but not too close to the endpoint ($m_b - 2E_0 \gg \Lambda_{\text{QCD}}$).

Conventionally, $E_0 = 1.6 \text{ GeV} \simeq m_b/3$ is chosen.

Updated SM estimate for the CP- and isospin-averaged
branching ratio of $\bar{B} \rightarrow X_s \gamma$ [arXiv:1503.01789, arXiv:1503.01791]:

$$\mathcal{B}_{s\gamma}^{\text{SM}} = (3.36 \pm 0.23) \times 10^{-4} \quad \text{for } E_\gamma > 1.6 \text{ GeV}$$

$\pm 6.9\%$

Contributions to the total TH uncertainty (summed in quadrature):

5% non-perturbative, **3%** from the interpolation in m_c

3% higher order $\mathcal{O}(\alpha_s^3)$, **2%** parametric

Updated SM estimate for the CP- and isospin-averaged
branching ratio of $\bar{B} \rightarrow X_s \gamma$ [arXiv:1503.01789, arXiv:1503.01791]:

$$\mathcal{B}_{s\gamma}^{\text{SM}} = (3.36 \pm 0.23) \times 10^{-4} \quad \text{for } E_\gamma > 1.6 \text{ GeV}$$

$\pm 6.9\%$

Contributions to the total TH uncertainty (summed in quadrature):

5% non-perturbative, **3%** from the interpolation in m_c

3% higher order $\mathcal{O}(\alpha_s^3)$, **2%** parametric

It is very close to the experimental world average:

$$\mathcal{B}_{s\gamma}^{\text{exp}} = (3.32 \pm 0.15) \times 10^{-4} \quad [\text{HFAG, arXiv:1612.07233}]$$

$\pm 4.5\%$

Experiment agrees with the SM well within $\sim \mathbf{1\sigma}$.

Updated SM estimate for the CP- and isospin-averaged
branching ratio of $\bar{B} \rightarrow X_s \gamma$ [arXiv:1503.01789, arXiv:1503.01791]:

$$\mathcal{B}_{s\gamma}^{\text{SM}} = (3.36 \pm 0.23) \times 10^{-4} \quad \text{for } E_\gamma > 1.6 \text{ GeV}$$

$\pm 6.9\%$

Contributions to the total TH uncertainty (summed in quadrature):

5% non-perturbative, **3%** from the interpolation in m_c

3% higher order $\mathcal{O}(\alpha_s^3)$, **2%** parametric

It is very close the the experimental world average:

$$\mathcal{B}_{s\gamma}^{\text{exp}} = (3.32 \pm 0.15) \times 10^{-4} \quad [\text{HFAG, arXiv:1612.07233}]$$

$\pm 4.5\%$

Experiment agrees with the SM well within $\sim \mathbf{1\sigma}$.

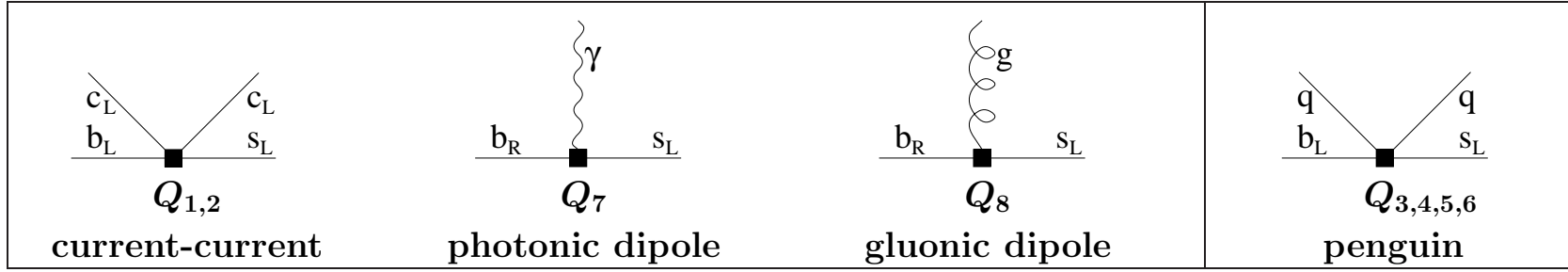
\Rightarrow Strong bound on the H^\pm mass in the Two-Higgs-Doublet-Model II:

$$M_{H^\pm} > 580 \text{ GeV at } 95\% \text{C.L.} \quad [\text{MM, M. Steinhauser, EPJC 77 (2017) 201}]$$

Decoupling of $W, Z, t, H^0 \Rightarrow$ effective weak interaction Lagrangian:

$$L_{\text{weak}} \sim \sum_i C_i Q_i$$

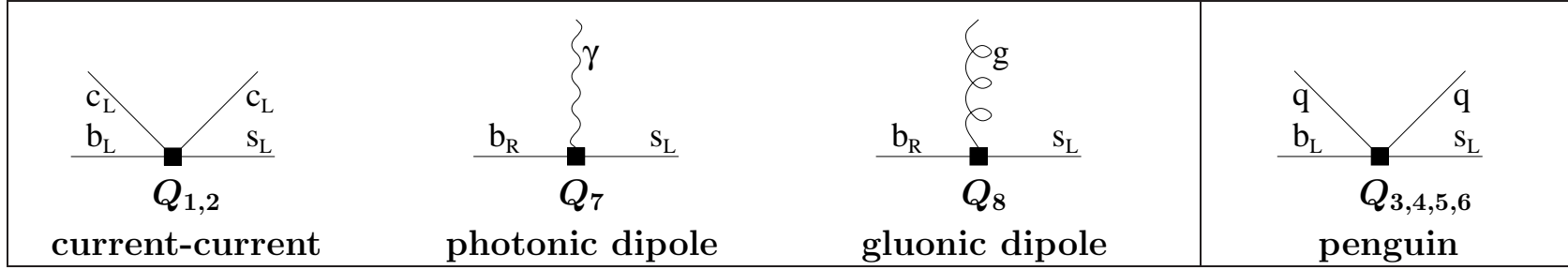
Eight operators Q_i matter for $\mathcal{B}_{s\gamma}^{\text{SM}}$ when the NLO EW and/or CKM-suppressed effects are neglected:



Decoupling of $W, Z, t, H^0 \Rightarrow$ effective weak interaction Lagrangian:

$$L_{\text{weak}} \sim \sum_i C_i Q_i$$

Eight operators Q_i matter for $\mathcal{B}_{s\gamma}^{\text{SM}}$ when the NLO EW and/or CKM-suppressed effects are neglected:

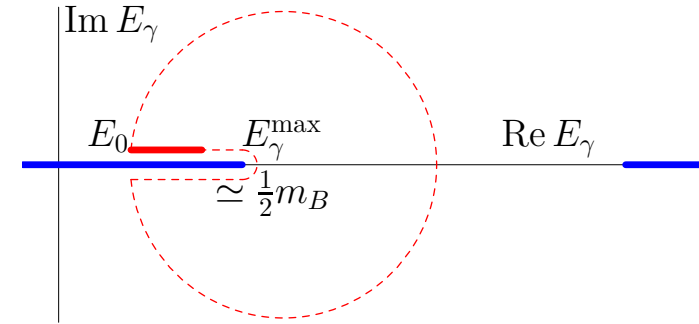


$$\Gamma(\bar{B} \rightarrow X_s \gamma)_{E_\gamma > E_0} = |C_7(\mu_b)|^2 \Gamma_{77}(E_0) + (\text{other}) \quad (\mu_b \sim m_b/2)$$

Optical theorem:

Integrating the amplitude A over E_γ :

$$\frac{d\Gamma_{77}}{dE_\gamma} \sim \text{Im} \left\{ \bar{B} \begin{array}{c} \text{---} \gamma \text{---} \\ \text{---} X_s \text{---} \\ \text{---} \end{array} \bar{B} \right\} \equiv \text{Im} A$$



OPE on the ring \Rightarrow Non-perturbative corrections to $\Gamma_{77}(E_0)$ form a series in $\frac{\Lambda_{\text{QCD}}}{m_b}$ and α_s that begins with

$$\frac{\mu_\pi^2}{m_b^2}, \frac{\mu_G^2}{m_b^2}, \frac{\rho_D^3}{m_b^3}, \frac{\rho_{LS}^3}{m_b^3}, \dots; \frac{\alpha_s \mu_\pi^2}{(m_b - 2E_0)^2}, \frac{\alpha_s \mu_G^2}{m_b(m_b - 2E_0)}; \dots,$$

where $\mu_\pi, \mu_G, \rho_D, \rho_{LS} = \mathcal{O}(\Lambda_{\text{QCD}})$ are extracted from the semileptonic $\bar{B} \rightarrow X_c e \bar{\nu}$ spectra and the $B-B^*$ mass difference.

NNLO QCD corrections to $\bar{B} \rightarrow X_s \gamma$

The relevant perturbative quantity $P(E_0)$:

$$\frac{\Gamma[b \rightarrow X_s \gamma]_{E_\gamma > E_0}}{\Gamma[b \rightarrow X_u e \bar{\nu}]} = \left| \frac{V_{ts}^* V_{tb}}{V_{ub}} \right|^2 \frac{6\alpha_{\text{em}}}{\pi} \underbrace{\sum_{i,j} C_i(\mu_b) C_j(\mu_b) K_{ij}}_{P(E_0)}$$

NNLO QCD corrections to $\bar{B} \rightarrow X_s \gamma$

The relevant perturbative quantity $P(E_0)$:

$$\frac{\Gamma[b \rightarrow X_s \gamma]_{E_\gamma > E_0}}{\Gamma[b \rightarrow X_u e \bar{\nu}]} = \left| \frac{V_{ts}^* V_{tb}}{V_{ub}} \right|^2 \frac{6\alpha_{\text{em}}}{\pi} \underbrace{\sum_{i,j} C_i(\mu_b) C_j(\mu_b) K_{ij}}_{P(E_0)}$$

Expansions of the Wilson coefficients and K_{ij} in $\tilde{\alpha}_s \equiv \frac{\alpha_s(\mu_b)}{4\pi}$:

$$C_i(\mu_b) = C_i^{(0)} + \tilde{\alpha}_s C_i^{(1)} + \tilde{\alpha}_s^2 C_i^{(2)} + \dots$$

$$K_{ij} = K_{ij}^{(0)} + \tilde{\alpha}_s K_{ij}^{(1)} + \tilde{\alpha}_s^2 K_{ij}^{(2)} + \dots$$

NNLO QCD corrections to $\bar{B} \rightarrow X_s \gamma$

The relevant perturbative quantity $P(E_0)$:

$$\frac{\Gamma[b \rightarrow X_s \gamma]_{E_\gamma > E_0}}{\Gamma[b \rightarrow X_u e \bar{\nu}]} = \left| \frac{V_{ts}^* V_{tb}}{V_{ub}} \right|^2 \frac{6\alpha_{\text{em}}}{\pi} \underbrace{\sum_{i,j} C_i(\mu_b) C_j(\mu_b) K_{ij}}_{P(E_0)}$$

Expansions of the Wilson coefficients and K_{ij} in $\tilde{\alpha}_s \equiv \frac{\alpha_s(\mu_b)}{4\pi}$:

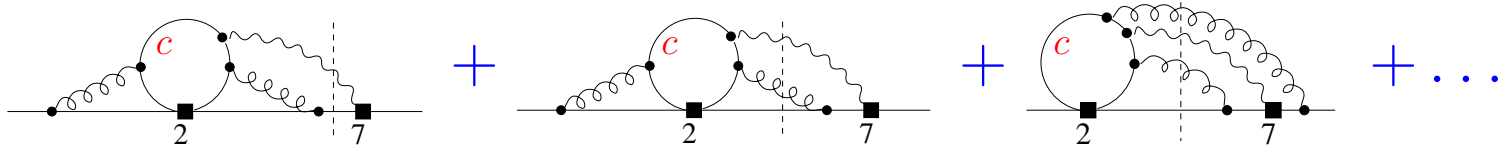
$$C_i(\mu_b) = C_i^{(0)} + \tilde{\alpha}_s C_i^{(1)} + \tilde{\alpha}_s^2 C_i^{(2)} + \dots$$

$$K_{ij} = K_{ij}^{(0)} + \tilde{\alpha}_s K_{ij}^{(1)} + \tilde{\alpha}_s^2 K_{ij}^{(2)} + \dots$$

Most important at the NNLO: $K_{77}^{(2)}$, $K_{27}^{(2)}$ and $K_{17}^{(2)}$.

They depend on $\frac{\mu_b}{m_b}$, $\delta = 1 - \frac{2E_0}{m_b}$ and $z = \frac{m_c^2}{m_b^2}$.

Towards complete $K_{17}^{(2)}$ and $K_{27}^{(2)}$ for arbitrary m_c [MM, A. Rehman, M. Steinhauser, ...] in progress



1. Generation of diagrams and performing the Dirac algebra to express everything in terms of 585309 **four-loop two-scale** scalar integrals with unitarity cuts (437 families).

2. Reduction to master integrals with the help of Integration By Parts (IBP).

Available public C++ codes: **REDUZE** [C. Studerus, arXiv:0912.2546],
FIRE [A.V. Smirnov, arXiv:1408.2372].

A useful Mathematica code: **LiteRed** [R.N. Lee, arXiv:1212.2685] (**symmetries...**).

At the moment (MM), 147 families (166509 integrals) still await for reduction.

Expected needs for the most difficult families: 100 GB RAM & 1 month CPU.

3. Extending the set of master integrals I_n so that it closes under differentiation with respect to $z = m_c^2/m_b^2$. This way one obtains a system of differential equations

$$\frac{d}{dz} I_n = \sum_k w_{nk}(z, \epsilon) I_k, \quad (*)$$

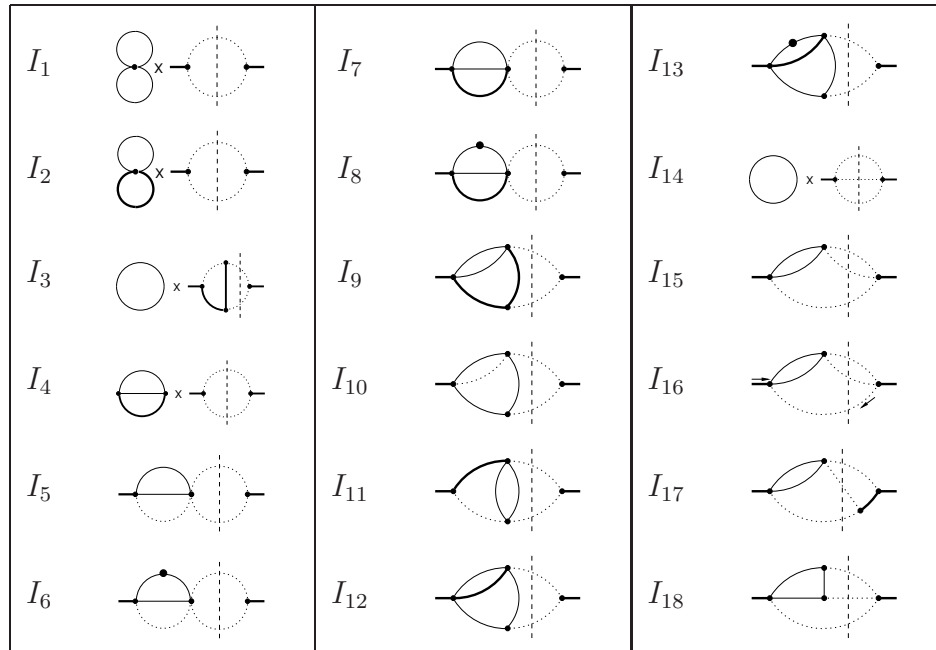
where w_{nk} are rational functions of their arguments.

4. Calculating boundary conditions for $(*)$ using automatized asymptotic expansions at $m_c \gg m_b$.
5. Calculating **three-loop single-scale** master integrals for the boundary conditions. **Methods ...**
6. Solving the system $(*)$ numerically [A.C. Hindmarch, <http://www.netlib.org/odepack>] along an ellipse in the complex z plane. Doing so along several different ellipses allows us to estimate the numerical error.

The same method has been applied to the 3-loop counterterm diagrams

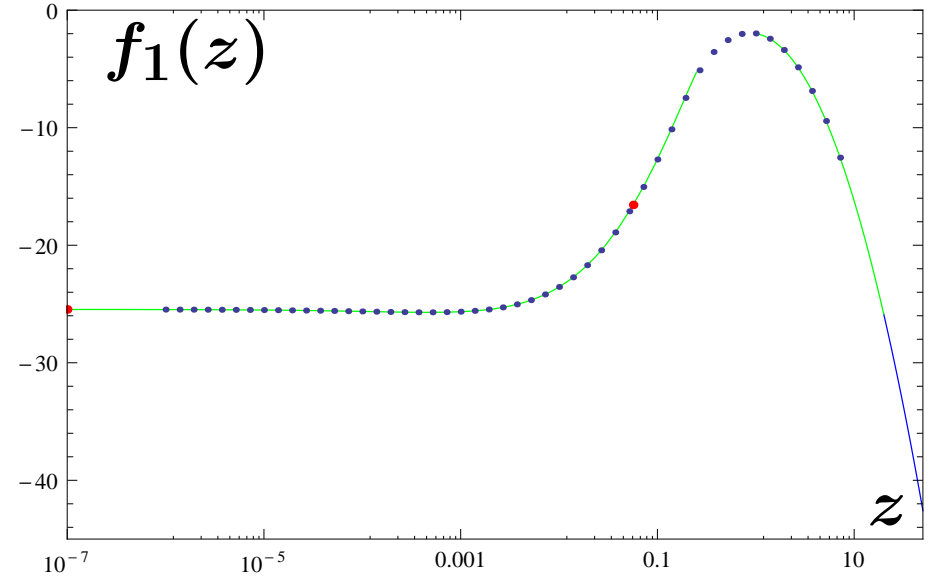
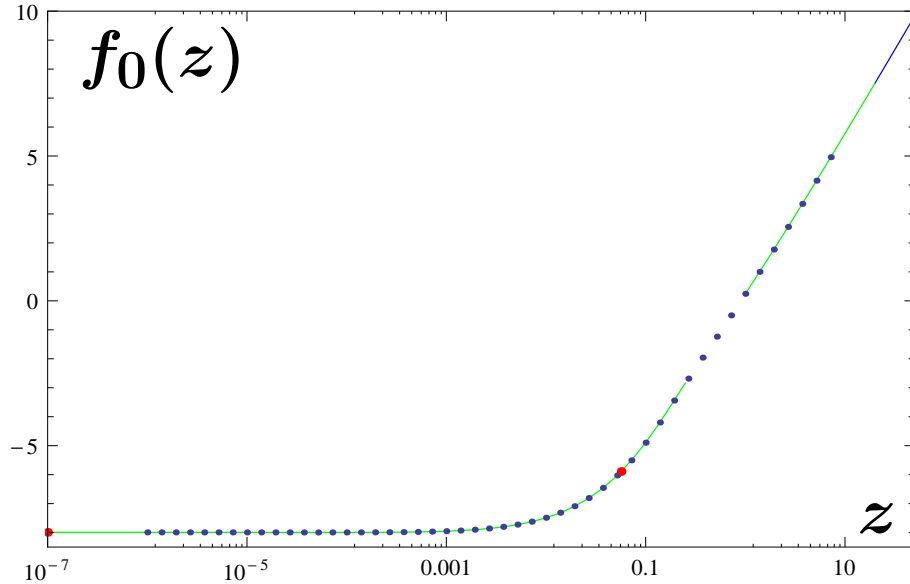
[MM, A. Rehman, M. Steinhauser, PLB 770 (2017) 431]

Master integrals:



Results for the bare NLO contributions up to $\mathcal{O}(\epsilon)$:

$$\hat{G}_{27}^{(1)2P} = -\frac{92}{81\epsilon} + f_0(z) + \epsilon f_1(z) \xrightarrow{z \rightarrow 0} -\frac{92}{81\epsilon} - \frac{1942}{243} + \epsilon \left(-\frac{26231}{729} + \frac{259}{243}\pi^2 \right)$$



Dots: solutions to the differential equations and/or the exact $z \rightarrow 0$ limit.

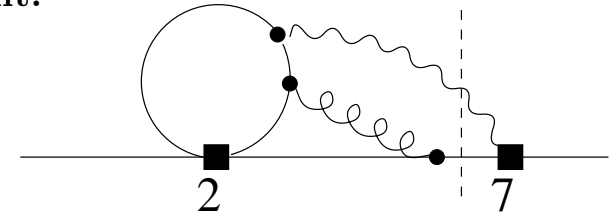
Lines: large- and small- z asymptotic expansions

Small- z expansions of $\hat{G}_{27}^{(1)2P}$:

f_0 from C. Greub, T. Hurth, D. Wyler, hep-ph/9602281, hep-ph/9603404,

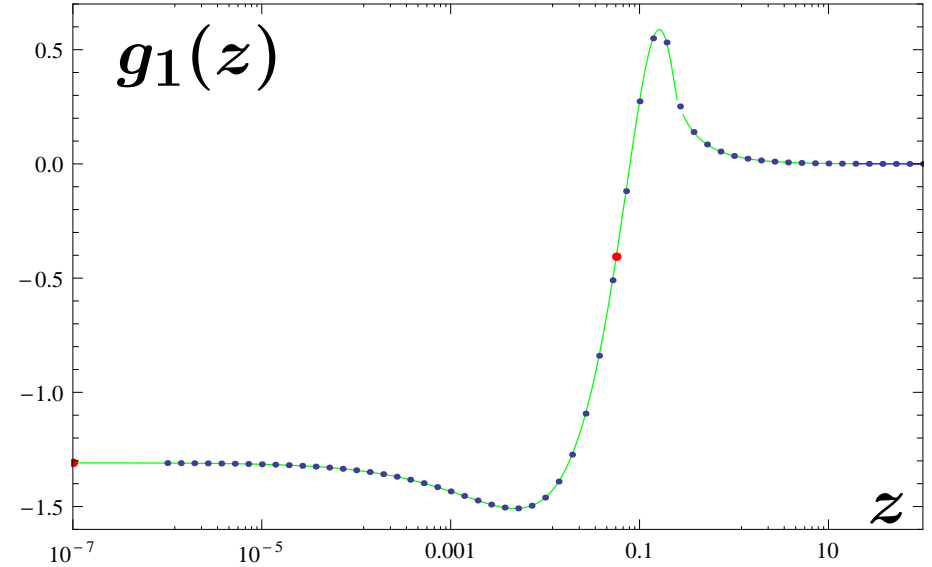
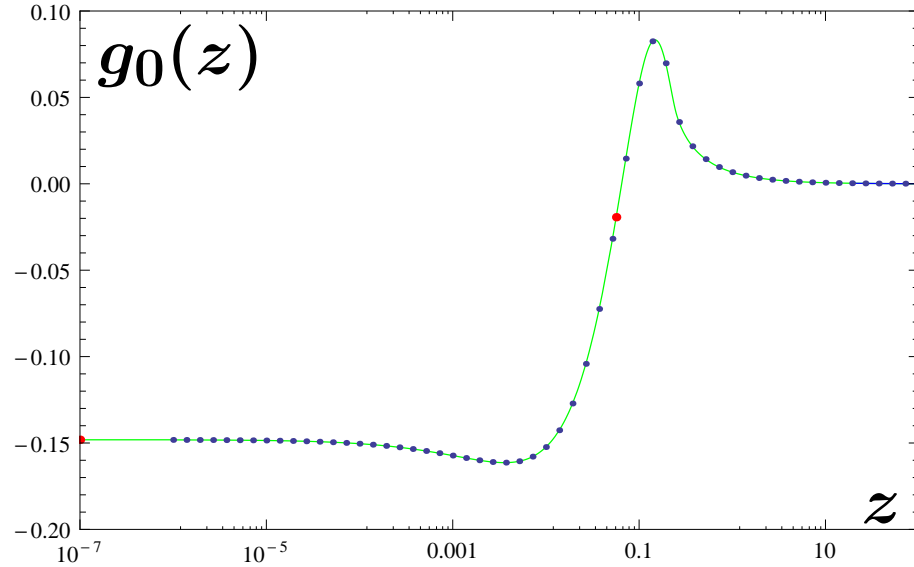
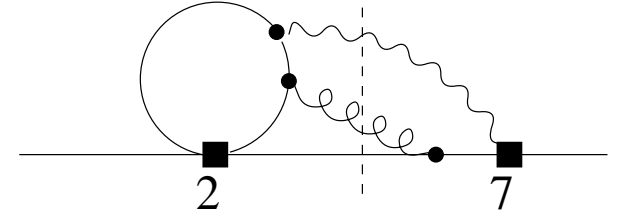
A. J. Buras, A. Czarnecki, MM, J. Urban, hep-ph/0105160,

f_1 from H.M. Asatrian, C. Greub, A. Hovhannisyanyan, T. Hurth and V. Poghosyan, hep-ph/0505068.



Analogous results for the 3-body final state contributions ($\delta = 1$):

$$\hat{G}_{27}^{(1)3P} = g_0(z) + \epsilon g_1(z) \xrightarrow{z \rightarrow 0} -\frac{4}{27} - \frac{106}{81}\epsilon$$



Dots: solutions to the differential equations and/or the exact $z \rightarrow 0$ limit.

Lines: exact result for g_0 , as well as large- and small- z asymptotic expansions for g_1 .

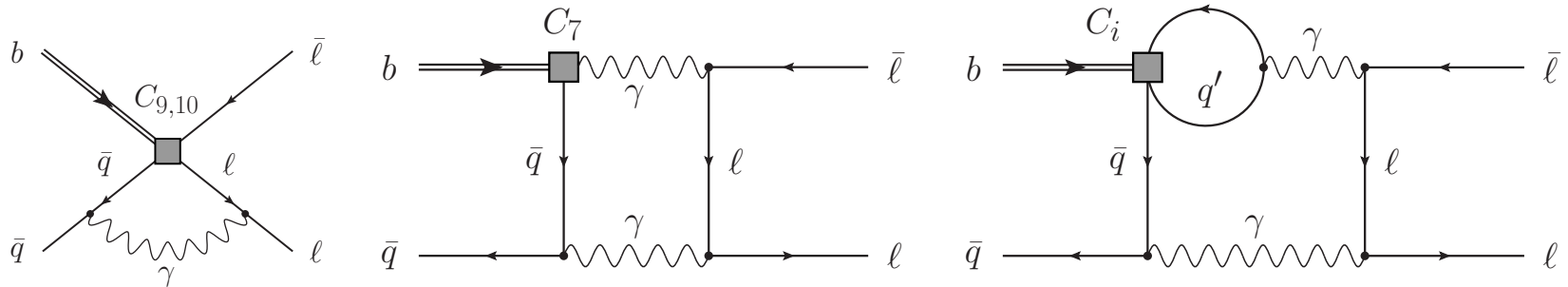
$$g_0(z) = \begin{cases} -\frac{4}{27} - \frac{14}{9}z + \frac{8}{3}z^2 + \frac{8}{3}z(1-2z)sL + \frac{16}{9}z(6z^2-4z+1)\left(\frac{\pi^2}{4} - L^2\right), & \text{for } z \leq \frac{1}{4}, \\ -\frac{4}{27} - \frac{14}{9}z + \frac{8}{3}z^2 + \frac{8}{3}z(1-2z)tA + \frac{16}{9}z(6z^2-4z+1)A^2, & \text{for } z > \frac{1}{4}, \end{cases}$$

where $s = \sqrt{1-4z}$, $L = \ln(1+s) - \frac{1}{2}\ln 4z$, $t = \sqrt{4z-1}$, and $A = \arctan(1/t)$.

Enhanced QED effects in $B_q \rightarrow \ell^+ \ell^-$

The leading contribution to the decay rate is proportional to $f_{B_q}^2 \sim \frac{\Lambda^3}{M_{B_q}}$.

As observed by M. Beneke, C. Bobeth and R. Szafron in arXiv:1708.09152, some of the QED corrections scale like Λ^2 :



Consequently, the relative QED correction scales like $\frac{\alpha_{em}}{\pi} \frac{M_{B_q}}{\Lambda}$.

Their explicit calculation implies that the previous results for all the $B_q \rightarrow \ell^+ \ell^-$ branching ratios need to be multiplied by

$$0.993 \pm 0.004.$$

Thus, despite the $\frac{M_{B_q}}{\Lambda}$ -enhancement, the effect is well within the previously estimated $\pm 1.5\%$ non-parametric uncertainty.

However, it is larger than $\pm 0.3\%$ stemming from scale-variation of the Wilson coefficient $C_A(\mu_b)$.

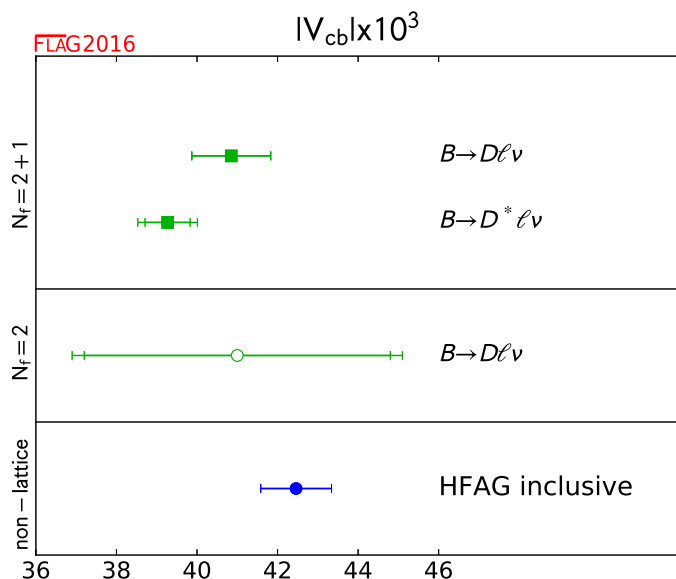
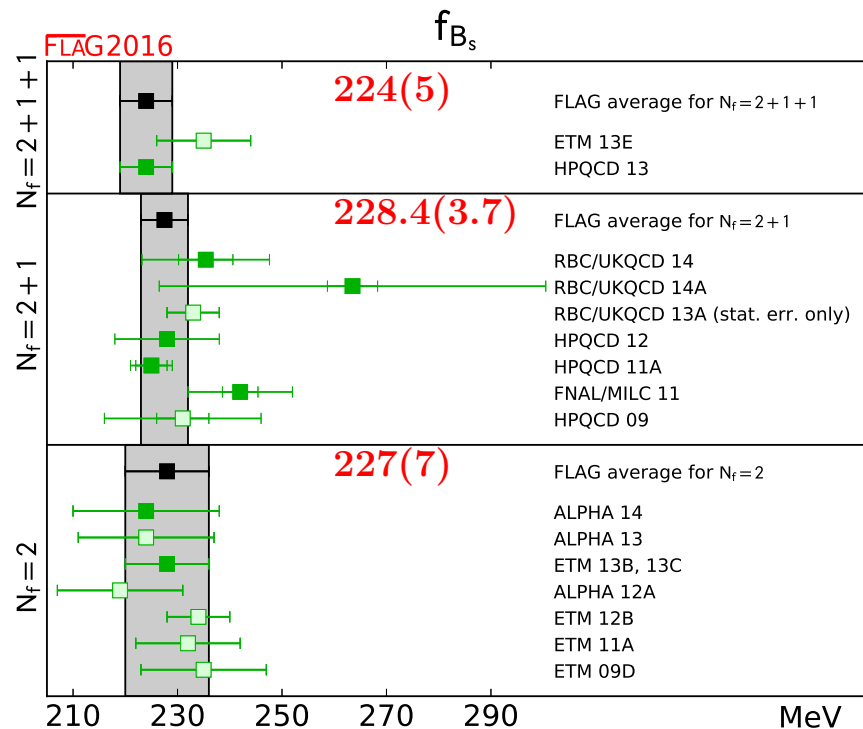
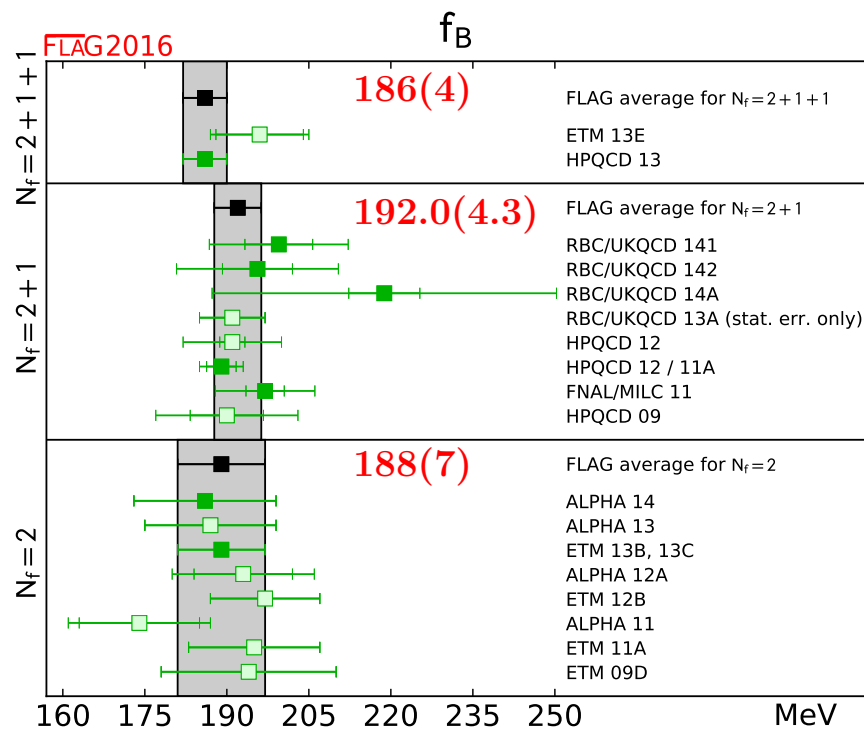
SM predictions for all the branching ratios $\overline{\mathcal{B}}_{q\ell} \equiv \overline{\mathcal{B}}(B_q^0 \rightarrow \ell^+ \ell^-)$

[C. Bobeth, M. Gorbahn, T. Hermann, MM, E. Stamou, M. Steinhauser, PRL 112 (2014) 101801]

$$\begin{aligned}
\overline{\mathcal{B}}_{se} \times 10^{14} &= (8.54 \pm 0.13) R_{t\alpha} R_s, \\
\overline{\mathcal{B}}_{s\mu} \times 10^9 &= (3.65 \pm 0.06) R_{t\alpha} R_s, \\
\overline{\mathcal{B}}_{s\tau} \times 10^7 &= (7.73 \pm 0.12) R_{t\alpha} R_s, \\
\overline{\mathcal{B}}_{de} \times 10^{15} &= (2.48 \pm 0.04) R_{t\alpha} R_d, \\
\overline{\mathcal{B}}_{d\mu} \times 10^{10} &= (1.06 \pm 0.02) R_{t\alpha} R_d, \\
\overline{\mathcal{B}}_{d\tau} \times 10^8 &= (2.22 \pm 0.04) R_{t\alpha} R_d,
\end{aligned}$$

where

$$\begin{aligned}
R_{t\alpha} &= \left(\frac{M_t}{173.1 \text{ GeV}} \right)^{3.06} \left(\frac{\alpha_s(M_Z)}{0.1184} \right)^{-0.18}, \\
R_s &= \left(\frac{f_{B_s} [\text{MeV}]}{227.7} \right)^2 \left(\frac{|V_{cb}|}{0.0424} \right)^2 \left(\frac{|V_{tb}^* V_{ts}/V_{cb}|}{0.980} \right)^2 \frac{\tau_H^s [\text{ps}]}{1.615}, \\
R_d &= \left(\frac{f_{B_d} [\text{MeV}]}{190.5} \right)^2 \left(\frac{|V_{tb}^* V_{td}|}{0.0088} \right)^2 \frac{\tau_d^{\text{av}} [\text{ps}]}{1.519}.
\end{aligned}$$



0.041(1)

0.03927(76) (2.7 σ tension with the inclusive)

→ 0.04200(64) from P. Gambino, K. J. Healey and S. Turczyk
Phys.Lett.B 763 (2016) 60.

Update of the input parameters

| | 2014 paper | this talk | source |
|--|-------------|-------------|-----------------------------|
| M_t [GeV] | 173.1(9) | 174.30(65) | CDF & D0, arXiv:1608.01881 |
| $\alpha_s(M_Z)$ | 0.1184(7) | 0.1182(12) | PDG 2016 |
| f_{B_s} [GeV] | 0.2277(45) | 0.2240(50) | FLAG 2016 |
| f_{B_d} [GeV] | 0.1905(42) | 0.1860(40) | FLAG 2016 |
| $ V_{cb} $ | 0.04240(90) | 0.04089(44) | naive average excl. & incl. |
| $ V_{tb}^* V_{ts} / V_{cb} $ | 0.9800(10) | 0.9819(4) | derived from CKMfitter 2016 |
| $ V_{tb}^* V_{td} $ | 0.0088(3) | 0.0087(2) | derived from CKMfitter 2016 |
| τ_H^s [ps] | 1.615(21) | 1.619(9) | HFLAV 2017 |
| τ_H^d [ps] | 1.519(7) | 1.518(4) | HFLAV 2017 |
| $\overline{\mathcal{B}}_{s\mu} \times 10^9$ | 3.65(23) | 3.35(18) | |
| $\overline{\mathcal{B}}_{d\mu} \times 10^{10}$ | 1.06(9) | 1.00(7) | |

| Sources of uncertainties | f_{B_q} | CKM | τ_H^q | M_t | α_s | other parametric | non-parametric | Σ |
|----------------------------------|-----------|------|------------|-------|------------|------------------|----------------|----------|
| $\overline{\mathcal{B}}_{s\ell}$ | 4.5% | 2.2% | 0.6% | 1.2% | 0.1% | < 0.1% | 1.5% | 5.4% |
| $\overline{\mathcal{B}}_{d\ell}$ | 4.3% | 4.6% | 0.3% | 1.2% | 0.1% | < 0.1% | 1.5% | 6.7% |

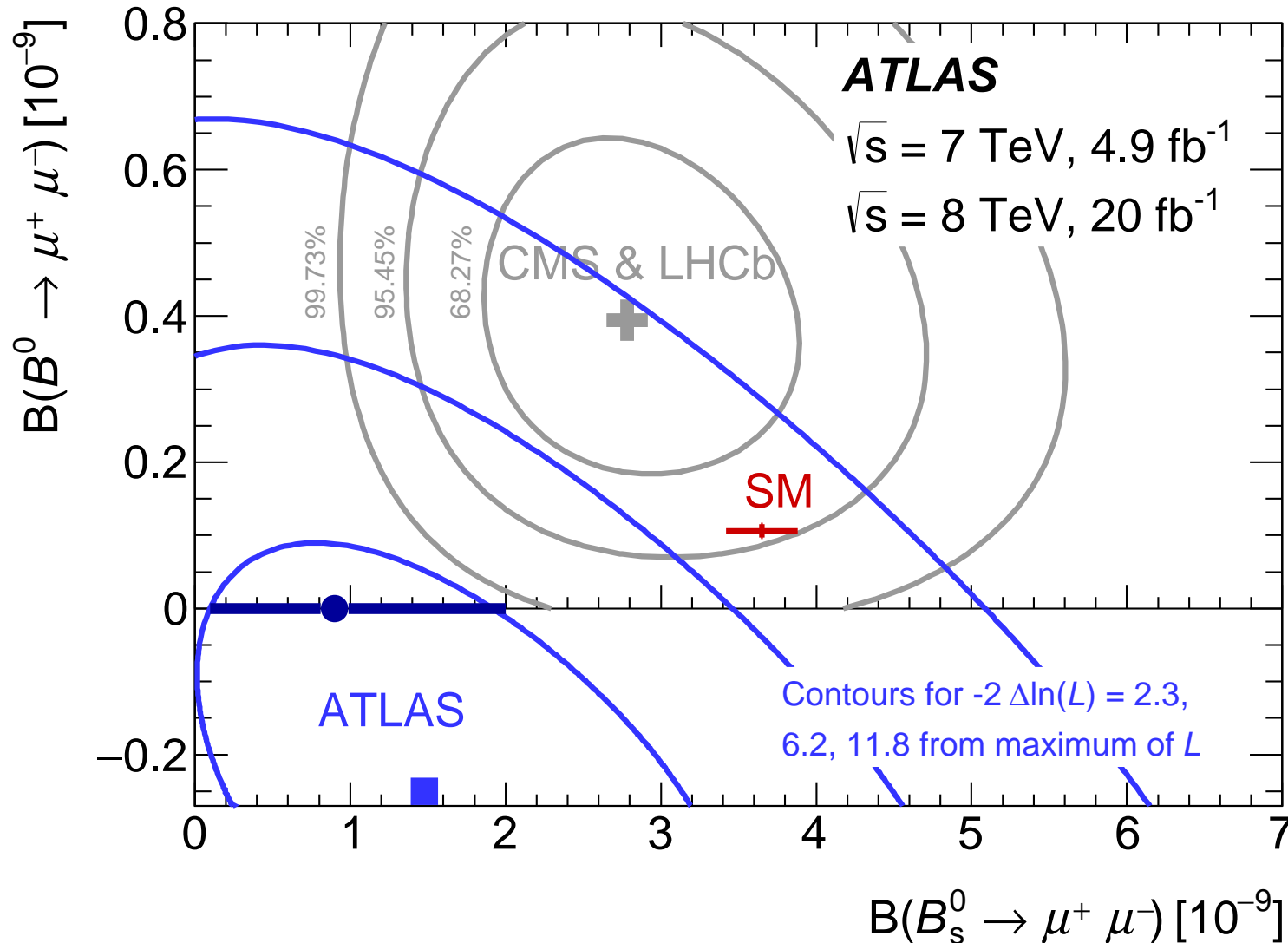
If the inclusive $|V_{cb}| = 0.04200(64)$ alone is used instead of the naive average, then $\overline{\mathcal{B}}_{s\mu} \times 10^9 = 3.54(21)$.

Comparison with the measurements

Previous averages, CMS and LHCb, Nature 522 (2015) 68: $\overline{\mathcal{B}}_{s\mu} = (2.8^{+0.7}_{-0.6}) \times 10^{-9}$, $\overline{\mathcal{B}}_{d\mu} = (3.9^{+1.6}_{-1.4}) \times 10^{-10}$.

New results of LHCb, PRL 118 (2017) 191801: $\overline{\mathcal{B}}_{s\mu} = (3.0 \pm 0.6^{+0.3}_{-0.2}) \times 10^{-9}$, $\overline{\mathcal{B}}_{d\mu} = (1.5^{+1.2+0.2}_{-1.0-0.1}) \times 10^{-10}$.

ATLAS in EPJC 76 (2016) 513 gives 95% C.L. bounds: $\overline{\mathcal{B}}_{s\mu} < 3.0 \times 10^{-9}$ and $\overline{\mathcal{B}}_{d\mu} < 4.2 \times 10^{-10}$.

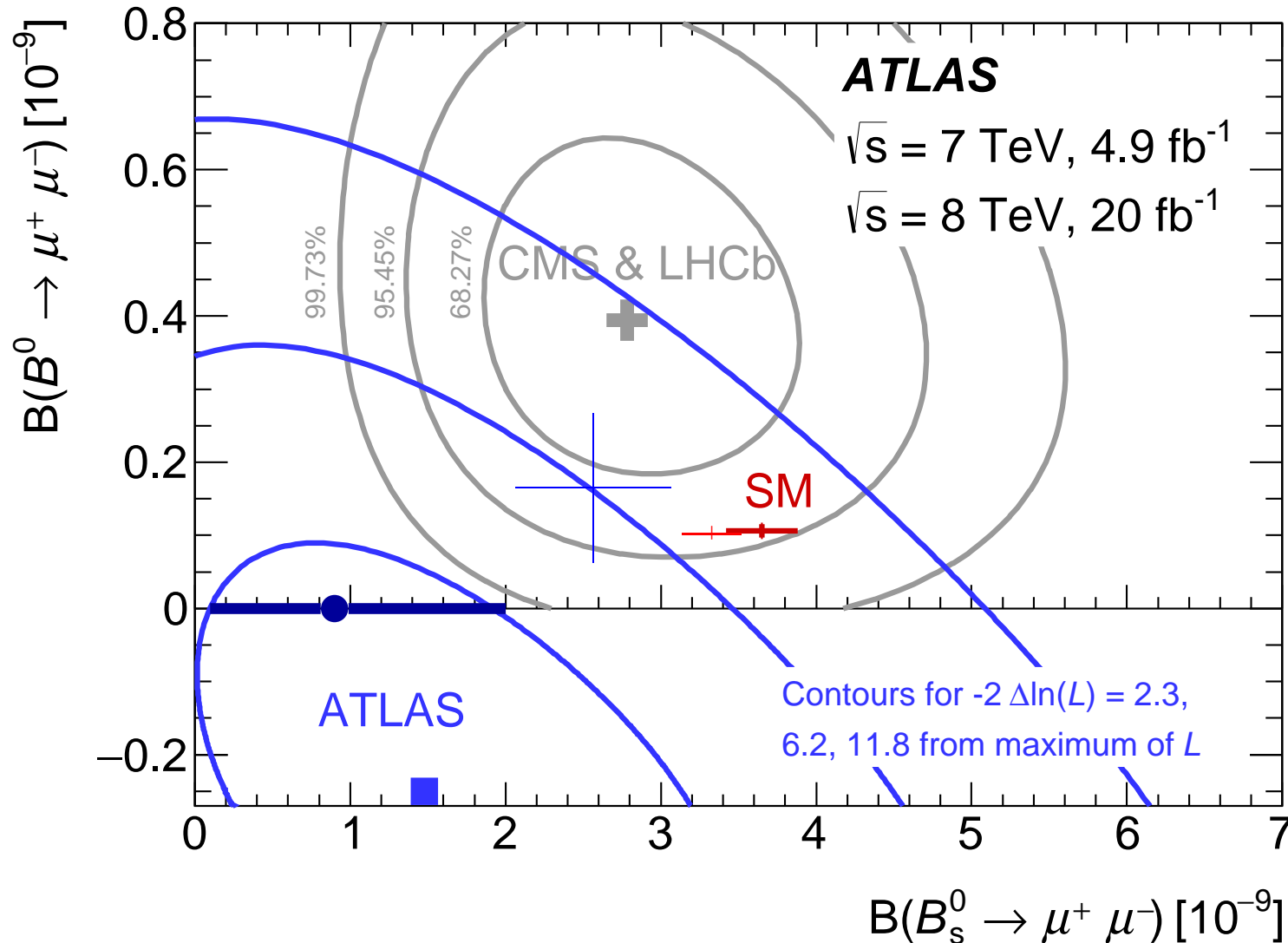


Comparison with the measurements

Previous averages, CMS and LHCb, Nature 522 (2015) 68: $\overline{\mathcal{B}}_{s\mu} = (2.8^{+0.7}_{-0.6}) \times 10^{-9}$, $\overline{\mathcal{B}}_{d\mu} = (3.9^{+1.6}_{-1.4}) \times 10^{-10}$.

New results of LHCb, PRL 118 (2017) 191801: $\overline{\mathcal{B}}_{s\mu} = (3.0 \pm 0.6^{+0.3}_{-0.2}) \times 10^{-9}$, $\overline{\mathcal{B}}_{d\mu} = (1.5^{+1.2+0.2}_{-1.0-0.1}) \times 10^{-10}$.

ATLAS in EPJC 76 (2016) 513 gives 95% C.L. bounds: $\overline{\mathcal{B}}_{s\mu} < 3.0 \times 10^{-9}$ and $\overline{\mathcal{B}}_{d\mu} < 4.2 \times 10^{-10}$.



Non-local charm loops in $\bar{B} \rightarrow X_s \gamma$ and $\bar{B} \rightarrow X_s \ell^+ \ell^-$

Background-subtracted $\bar{B} \rightarrow X_{s+d} \gamma$ photon energy spectrum in the $\Upsilon(4S)$ rest frame, from Fig. 1 of the Belle analysis in arXiv:1608.02344.

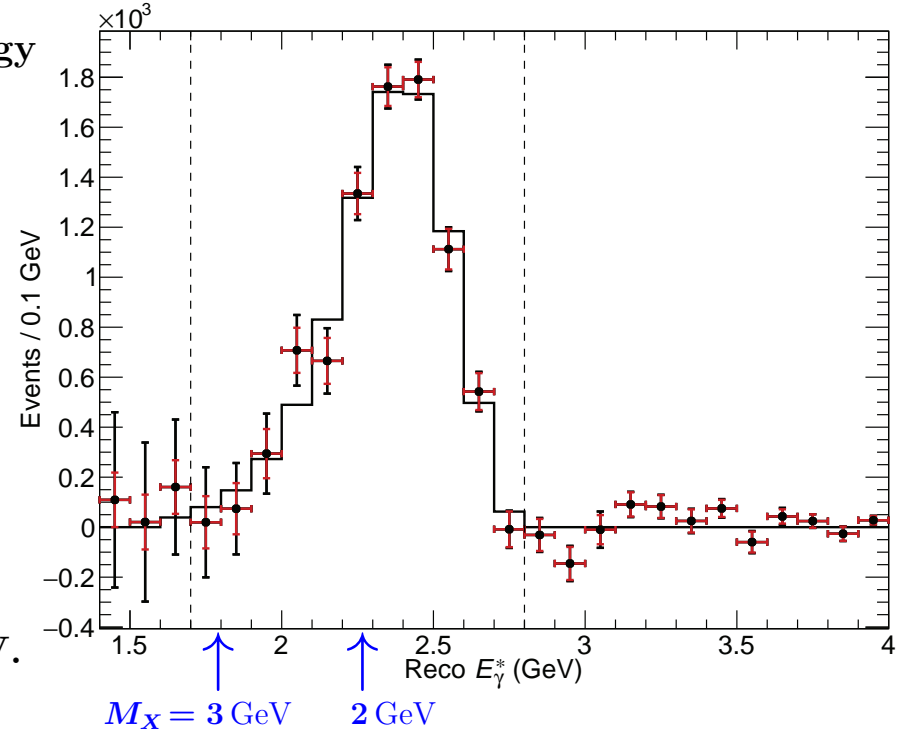
For $M_X \lesssim 3 \text{ GeV}$ and in the absence of 4-quark ops, we have local OPE $\Rightarrow \mathcal{O}(\Lambda^2/m_b^2)$.

In the presence of 4-quark ops:

Light quark loops – suppressed by $C_{3,\dots,6}$ or CKM;

Charm loops – factorizable or local if m_c^2 is sufficiently large w.r.t. $m_b \Lambda$. Numerically, $\mathcal{O}(3\%)$ non-fact. effects found in $\mathcal{B}(\bar{B} \rightarrow X_s \gamma)$ and $\mathcal{B}(\bar{B} \rightarrow X_s \ell^+ \ell^-)$ with $q^2 \in [1, 6] \text{ GeV}^2$.

[Buchalla, Isidori, Rey, NPB 511 (1998) 594]



However, m_c^2 is not sufficiently large \Rightarrow Treat it as $\mathcal{O}(m_b \Lambda)$ and use SCET, so far up to $\mathcal{O}(\Lambda/m_b)$:

For $\mathcal{B}(\bar{B} \rightarrow X_s \gamma)$ with $E_\gamma > 1.6 \text{ GeV}$ [Benzke, Lee, Neubert, Paz, JHEP 1008 (2010) 099] $[-4.8\%, +5.6\%]$ uncert. range.

For $\mathcal{B}(\bar{B} \rightarrow X_s \ell^+ \ell^-)$ with $q^2 \in [1, 6] \text{ GeV}^2$ [Benzke, Hurth, Turczyk, JHEP 1710 (2017) 031] $[-2.7\%, +1.8\%]$ range.

(On the top of the factorizable and/or local effects, including the Λ^2/m_c^2 ones.)

Corrections not involving Q_7 and Q_8 are of higher order, i.e. $\mathcal{O}\left[\left(\frac{\Lambda}{m_b}\right)^a\right]$ with $a \geq \frac{3}{2}$ and/or $\mathcal{O}\left(\frac{\alpha_s \Lambda}{m_b}\right)$.

That's what we miss using the purely perturbative expression for $|C_9^{\text{eff}}(q^2)|^2$ and the local $1/m_c^2$ effects.

However, the applied SCET power counting works only for small M_X and small q^2 – verte.

SCET power counting in the $\bar{B} \rightarrow X_s \ell^+ \ell^-$ analysis of [Benzke, Hurth and Turczyk, JHEP 1710 \(2017\) 031](#).

$$\lambda = \frac{\Lambda}{M_B}, \quad M_X \lesssim \sqrt{M_B \Lambda} = M_B \sqrt{\lambda} \sim m_c.$$

$$a^\mu = \frac{1}{2}(na)\bar{n}^\mu + \frac{1}{2}(\bar{n}a)n^\mu + a_\perp^\mu, \quad \text{with} \quad n^\mu = \begin{bmatrix} 1 \\ 0 \\ 0 \\ 1 \end{bmatrix}^\mu, \quad \bar{n}^\mu = \begin{bmatrix} 1 \\ 0 \\ 0 \\ -1 \end{bmatrix}^\mu$$

\uparrow
any vector

In the plot $q_\perp = 0 \Rightarrow q^2 = (\bar{n}q)(nq)$.

hard: $p \sim (1, 1, 1),$
hard-collinear: $p \sim (\lambda, 1, \sqrt{\lambda}),$
anti-hard-collinear: $p \sim (1, \lambda, \sqrt{\lambda}),$
soft: $p \sim (\lambda, \lambda, \lambda)$

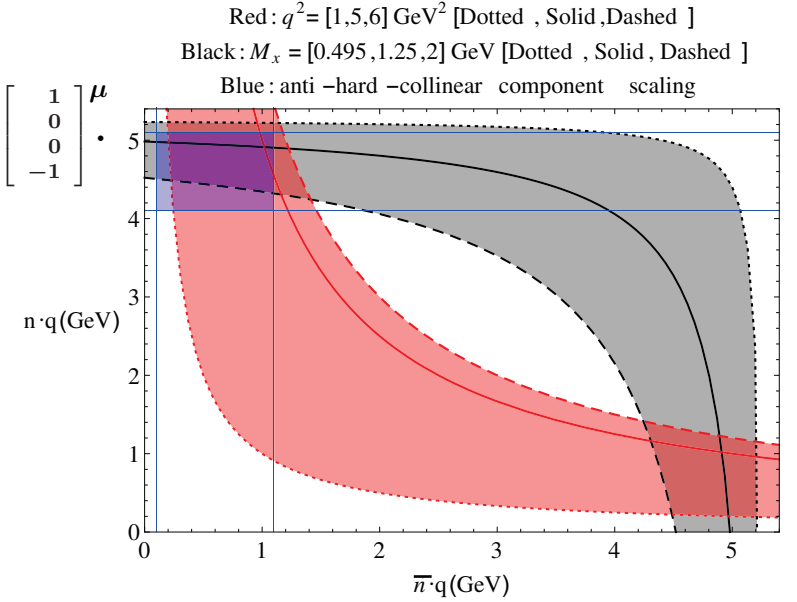
Plot \Rightarrow Our cuts would better fit into the SCET-accessible region if we restricted to $q^2 \in [1, 5] \text{ GeV}$. On the other hand, the cut on M_X could be somewhat larger than 2 GeV.

The factorization formula:

$$d\Gamma = \sum_{n=0}^{\infty} \frac{1}{m_b^n} \sum_i H_i^{(n)} J_i^{(n)} \otimes S_i^{(n)} + \sum_{n=1}^{\infty} \frac{1}{m_b^n} \left[\sum_i H_i^{(n)} J_i^{(n)} \otimes S_i^{(n)} \otimes \bar{J}_i^{(n)} + \sum_i H_i^{(n)} J_i^{(n)} \otimes S_i^{(n)} \otimes \bar{J}_i^{(n)} \otimes \bar{J}_i^{(n)} \right]$$

Remarks:

1. Not proven. Contradictions observed in the $Q_8 - Q_8$ case, claimed to be phenomenologically irrelevant.
2. Relates unknowns to unknowns. Models of soft functions needed (constraints available).
3. Corrections beyond $\mathcal{O}(\Lambda/m_b)$ are likely to be relevant because $|C_{9,10}/C_7| \sim 13$ (work in progress) [\[BHT\]](#).
4. Other observables – after including the above corrections.
5. Different power counting than in the previous SCET analyses where no "resolved photons" were included [\[Lee, Stewart, PRD74 \(2006\) 014005\]](#), [\[Bell, Beneke, Huber, Li, NPB843 \(2011\) 143\]](#).



Sample (previous) SM predictions for $\mathcal{B}(\bar{B} \rightarrow X_s \ell^+ \ell^-) \times 10^6$ with $q^2 \in [1, 6]$ GeV and no cut on M_X :

$$\left. \begin{array}{l} 1.64 \pm 0.11, \ell = e \\ 1.59 \pm 0.11, \ell = \mu \end{array} \right\} \text{parametric and perturbative uncert. only} \quad [\text{Huber, Lunghi, MM, Wyler, NPB 740 (2006) 105}]$$

$$\left. \begin{array}{l} 1.67 \pm 0.10, \ell = e \\ 1.62 \pm 0.09, \ell = \mu \end{array} \right\} \text{param. update + Krüger-Sehgal,} \quad [\text{Huber, Hurth, Lunghi, JHEP 1506 (2015) 176}]$$

PLB380 (1996) 199
PRD55 (1997) 2799

The corresponding semi-inclusive experimental results, averaged over $\ell = e, \mu$:

$$1.60_{-0.39}^{+0.41+0.17} \pm 0.18, \quad \text{Babar, PRL112 (2014) 211802, } 471 \times 10^6 B\bar{B}, \text{ extrapolated from } M_X < 1.8 \text{ GeV,}$$

$$1.493 \pm 0.504_{-0.321}^{+0.411}, \quad \text{Belle, PRD72 (2005) 092005, } 152 \times 10^6 B\bar{B}.$$

Remarks:

1. The Krüger-Sehgal (factorizable) contribution should be retained even after the SCET estimates for the resolved photon contributions are included in the future. **What about $\mathcal{O}(\alpha_s)$?**
2. Given the presence of resolved photon contributions, neither $\bar{B} \rightarrow X_s \gamma$ nor $\bar{B} \rightarrow X_s \ell^+ \ell^-$ are useful for precise determination of the HQET parameters. The semileptonic observables alone should be sufficient.
3. Suggestion: use $M_X < 3 \text{ GeV}$ as a default cut to which the experimental $\bar{B} \rightarrow X_s \ell^+ \ell^-$ results are being extrapolated, similarly to $E_\gamma > 1.6 \text{ GeV}$ in the $\bar{B} \rightarrow X_s \gamma$ case. The leading shape function is identical in both processes.

Summary

- Large deviations from the SM are observed in tree-level LFU-violating observables $R_{D^{(*)}}$, as well as in the loop generated transition $b \rightarrow s \ell^+ \ell^-$. On the other hand, several sensitive loop processes like $\bar{B} \rightarrow X_s \gamma$ or $B_s \rightarrow \mu^+ \mu^-$ remain in good agreement with the SM. Certain leptoquark models can accommodate such a situation.
- Perturbative calculations of $\bar{B} \rightarrow X_s \gamma$ require further optimization of software/hardware for the IBP reduction.
- In the case of $B_s \rightarrow \mu^+ \mu^-$, resolving the inclusive-exclusive tension in $|V_{cb}|$ would help a lot.
- Charm quark loops in the inclusive $\bar{B} \rightarrow X_s \ell^+ \ell^-$ decay seem to be under better control than in the corresponding exclusive decay channels.